



## Room-temperature deposition of hydroxyapatite/antibiotic composite coatings by vacuum cold spraying for antibacterial applications

Deyan Li<sup>a,b</sup>, Yongfeng Gong<sup>a</sup>, Xiuyong Chen<sup>a,\*</sup>, Botao Zhang<sup>c</sup>, Haijun Zhang<sup>b</sup>, Peipeng Jin<sup>b</sup>, Hua Li<sup>a,\*</sup>

<sup>a</sup> Key Laboratory of Marine Materials and Related Technologies, Key Laboratory of Marine Materials and Protective Technologies of Zhejiang Province, Ningbo Institute of Materials Technology and Engineering, Chinese Academy of Sciences, Ningbo 315201, China

<sup>b</sup> School of Mechanical Engineering, Qinghai University, Xining 810016, China

<sup>c</sup> Cixi Institute of Biomedical Engineering, Institute of Materials Technology and Engineering, Chinese Academy of Sciences, Ningbo 315201, China

### ARTICLE INFO

#### Keywords:

Hydroxyapatite  
Antibiotic  
Nanocomposite coatings  
Vacuum cold spray  
Antibacterial property

### ABSTRACT

To develop implants with long-term antibacterial property, hydroxyapatite (HA)-gentamicin sulfate (GS) composite powder were synthesized and deposited onto titanium substrates by vacuum cold spraying at room temperature. The successful fabrication of the HA-GS composite powder and coatings was confirmed by transmission electron microscopy (TEM), field-emission scanning electron microscopy (FE-SEM), Fourier transform infrared spectroscopy (FTIR) and X-ray photoelectron spectroscopy (XPS) analysis, respectively. Gentamicin release kinetics, antibacterial property and biocompatibility were systematically investigated *in vitro*. Results indicate that we can effectively load the coating with antibiotic and the coating shows long-term antibacterial capacity. Moreover, the HA-GS composite coatings displayed excellent biocompatibility. The approach in this study provides an alternative to fabricate an efficient bioactive drug delivery system for biomedical applications.

### 1. Introduction

Bacteria-induced inflammatory reaction is one of the main factors that result in the failure of implantation [1–3]. To prevent bacterial infection, conventional methods including debridement, irrigation and systemic antibiotics therapy treatment are generally used [4]. Nevertheless, bacterial infection develops in as many as 5–33% of implant surgeries [5]. Local antibiotic therapy has become an effective way to prevent infection owing to high local antibiotic concentration and nontoxicity, providing sustained delivery of antibiotics right at the site of implantation [6–8].

It is well known that gentamicin sulfate (GS) has strong antibacterial effect towards both gram-positive and negative bacteria and a number of strains of mycoplasma [9,10]. Thus, it is commonly used to inhibit bacterial infection around the implant. To date, many platforms including both organic and inorganic materials have been reported to load drugs for local delivery of antibiotics, such as polymethylmethacrylate (PMMA) beads [11–13], polyethylene terephthalate [14], polycaprolactone fiber [4], graphene nanosheets [15], titania nanotubes [5,16,17], tricalcium phosphate [8,18] and hydroxyapatite [19]. Among them, hydroxyapatite (HA) has been widely used in orthopedic applications, due to its similarity in chemistry to

human skeletal bones and teeth [20,21]. Traditionally, plasma spray technology has been successfully utilized for HA coating construction in clinical applications [22]. However, the processes of plasma spray method which carried out at a very high temperature are not suitable for fabrication of composite coatings loaded with temperature sensitive drugs. In recent years, vacuum cold spraying (VCS) has been employed to fabricate temperature sensitive nanostructured coatings owing to its unique advantages of retaining the chemistry of the temperature sensitive materials [23–26]. Nevertheless, to the best of our knowledge, this is the first study that employs VCS to construct antibiotic loaded composite coatings for antibacterial applications.

Herein, we report a new technical route for preparing hydroxyapatite-antibiotic composite coatings by VCS at room temperature for local delivery of gentamicin. Microstructural and chemical composition characterization of the powder and coatings were performed. The kinetics release of gentamicin from the coatings and its effect on *Escherichia coli* (*E. coli*) adhesion were investigated. Furthermore, the biocompatibility of the coatings was also evaluated *in vitro*.

\* Corresponding authors.

E-mail addresses: [chenxiuyong@nimte.ac.cn](mailto:chenxiuyong@nimte.ac.cn) (X. Chen), [lihua@nimte.ac.cn](mailto:lihua@nimte.ac.cn) (H. Li).

<http://dx.doi.org/10.1016/j.surfcoat.2017.09.085>

Received 21 August 2017; Received in revised form 28 September 2017; Accepted 30 September 2017

Available online 02 October 2017

0257-8972/ © 2017 Elsevier B.V. All rights reserved.

## 2. Experimental part

### 2.1. Sample preparation

HA powder in nanosizes was synthesized using a wet chemical approach as previously described [20]. Briefly,  $(\text{NH}_4)_2\text{HPO}_4$  (purchased from Sinopharm Chemical Reagent Co., Ltd., China) was slowly dripped into the  $\text{Ca}(\text{NO}_3)_2 \cdot 4\text{H}_2\text{O}$  solution, followed by adjustment of the pH to 11 using  $\text{NH}_3 \cdot \text{H}_2\text{O}$ . The solution was then mechanically stirred for 2 h to complete reaction and settled overnight. The resulting slurry was thoroughly washed with distilled water to remove ammonium hydroxide and freeze dried for 24 h. HA-gentamicin sulfate (GS, Sinopharm Chemical Reagent Co., Ltd., China) composite powder were produced by adding HA powder to the GS solution, followed by freeze drying.

Titanium alloy (Ti-6Al-4V) with the dimension of  $10 \times 10 \times 1$  mm was used as the substrates. The VCS 2000 system (developed by Xi'an Jiaotong University, China) was used to deposit the HA and the HA-GS powder onto titanium substrates at room temperature according to previous studies [21,25,26]. Helium was used as the carrier gas with a flow rate of 5 L/min. The scanning speed was 10 mm/s and the spray distance was 10 mm.

### 2.2. Sample characterization

Microstructure of the powder and the coatings were characterized by transmission electron microscopy (TEM, FEI Tecnai F20, the Netherlands) and field emission scanning electron microscopy (FESEM, FEI Quanta FEG250, the Netherlands), respectively. The infrared spectra of the powder and the coatings were obtained by Fourier transform infrared spectroscopy (FTIR, Nicolet 6700, Thermo Fisher Scientific, USA) with a resolution of  $8 \text{ cm}^{-1}$  and a scan number of 4 at a spectral region ranging from 400 to  $4000 \text{ cm}^{-1}$ . Chemical composition of the powder and the coatings was detected using X-ray photoelectron spectroscopy (XPS, AXIS ULTRA DLD, Japan).

### 2.3. Cumulative release of GS

In order to investigate the release of GS from the HA-GS coatings, the samples were put in wells of a 6-well plate with 5 mL phosphate-buffered saline (PBS, Sinopharm Chemical Reagent Co., Ltd., China) and gently shaken at  $37^\circ\text{C}$ . At predetermined time intervals of 1, 3, 7, 14, 21, 28 and 31 days, the GS contained PBS solution was collected and fresh PBS was added to the wells. The GS contained PBS solution was analyzed using a UV-vis spectrophotometer (Lambda 950, Perkin Elmer, USA) at the wavelength of 248 nm.

### 2.4. Antibacterial assay

Gram-negative *E. coli* bacteria (ATCC25922), which have been widely used for antibacterial assay [2,15,27–30], were used as a simplified model to investigate the antibacterial effects of the samples. Native titanium substrates were used as control. Bacteria were initially cultured in LB media which was prepared by dissolving 5 g yeast extract, 10 g NaCl and 10 g peptone in 1000 mL deionized water. The

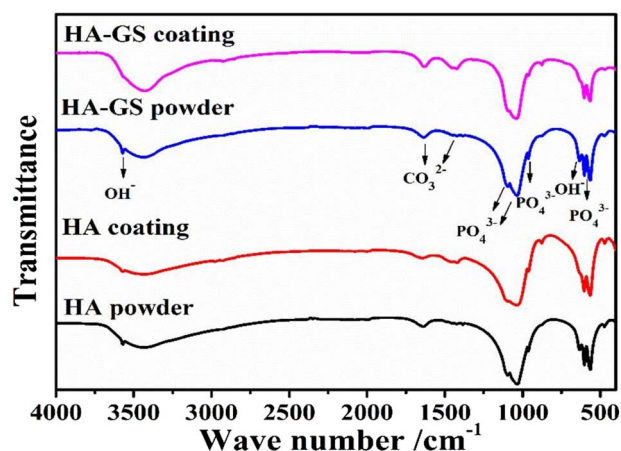


Fig. 2. FTIR spectra of the HA powder, the HA coating, the HA-GS powder and the HA-GS coating.

culture medium of nutrient agar was prepared by dissolving 33 g nutrient agar (Sinopharm Chemical Reagent Co., Ltd., China) in 1000 mL deionized water. And all samples were firstly sterilized by UV irradiated both sides for 120 min, respectively. For antibacterial rate assay [30], the HA coatings, the HA-GS coatings and the HA-GS coatings after immersed in PBS for 31 days (HA-GS(R) coating) were exposed to  $40 \mu\text{L}$  ( $10^6$  cells/mL) bacteria suspension and incubated at  $37^\circ\text{C}$ . *E. coli* adhered on the samples were removed with 4 mL PBS by vigorous shaking for 10 min.  $100 \mu\text{L}$  of the *E. coli* suspension of each sample was then spread onto nutrient agar plates and incubated at  $37^\circ\text{C}$  for 24 h. The number of colonies formed units (CFUs) was counted. The antibacterial rate was calculated according to the equation:  $A = \left( \frac{N_0 - N}{N_0} \right) \times 100\%$ , where A is the antibacterial rate;  $N_0$  is the CFUs of the uncoated titanium substrate; N is the CFUs of the coated titanium substrates.

### 2.5. Cell culture test

Attachment of the human osteoblast cells (HFOB 1.19 SV40 transfected osteoblasts) on the coating samples was examined. All samples were firstly sterilized by UV irradiated both sides overnight, respectively. Osteoblasts were cultured in a  $\alpha$ -minimum medium ( $\alpha$ -MEM) (SH30265.01B, HyClone, USA) supplemented with 10% heat-inactivated fetal bovine serum, 100 U/mL penicillin and 100  $\mu\text{g}/\text{mL}$  streptomycin in an atmosphere of 100% humidity and 5%  $\text{CO}_2$  at  $37^\circ\text{C}$ . Osteoblasts were seeded onto the sterilized samples at an initial density of  $1 \times 10^4$  cells/mL in 12-well culture plates with 1.5 mL media in each well. For SEM observation of osteoblasts adhesion on the surfaces of the samples, the cells after incubated for 1 day and 3 days were fixed with 2.5% glutaraldehyde for 24 h, and dehydrated through the critical point drying using 25%, 50%, 75%, 90%, and 100% ethanol solution. The dehydrated samples were finally sputter-coated with gold for SEM observation. Native titanium substrates were used as control.

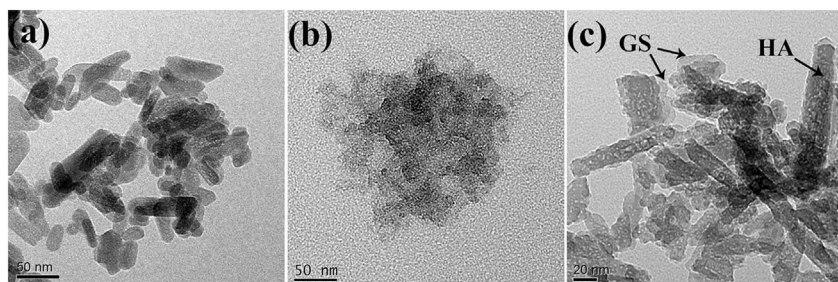


Fig. 1. TEM images of (a) the HA powder, (b) the GS powder and (c) the HA-GS composite powder.

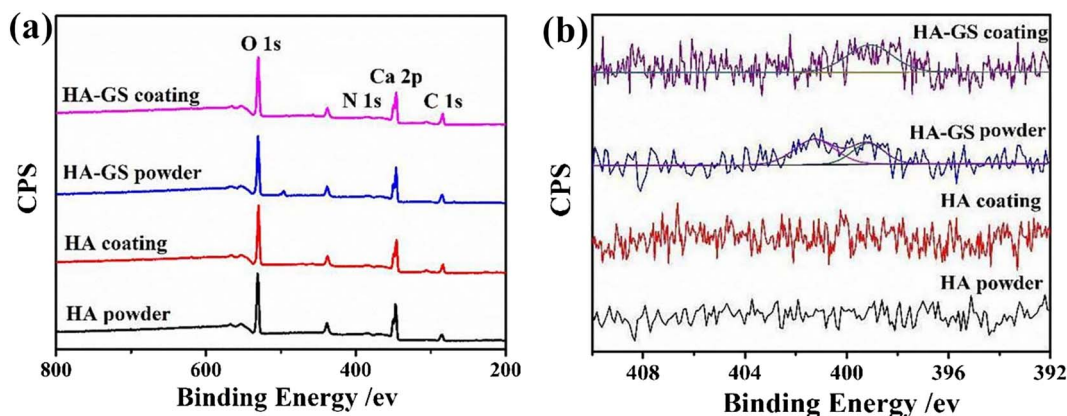


Fig. 3. XPS spectra of the powder and the coatings (a), and high resolution XPS spectra of N1 s (b).

Table 1  
XPS chemical compositions of the samples.

Samples	O (at. %)	N (at. %)	Ca (at. %)	C (at. %)
Ha powder	59.85	0	17.86	22.3
Ha coating	60.69	0	17.61	20.7
Ha-GS powder	57.46	1.03	17.11	24.4
Ha-GS coating	54.24	1.93	13.74	30.1

### 3. Results and discussion

#### 3.1. Characterization of the prepared powder and coatings

To prepare the HA-GS composite powder, the synthesized HA powder were dispersed in GS PBS solution and then dried. The morphologies of untreated and GS treated HA nanoparticles are shown in Fig. 1 a and c, respectively. The TEM image of the synthesized HA nanoparticles showed a rod-like shape with the size of ~20–100 nm in length and ~10 nm in diameter (Fig. 1 a). Clear surface modification is seen for the HA nanoparticles after the treatment with GS (Fig. 1 c). FTIR analyses of the HA powder and coating, and the HA-GS powder and coating are shown in Fig. 2. The peaks at 1093 cm<sup>-1</sup>, 1032 cm<sup>-1</sup>, 961 cm<sup>-1</sup>, 602 cm<sup>-1</sup>, 564 cm<sup>-1</sup> and 472 cm<sup>-1</sup> are attributed to the stretching vibration of PO<sub>4</sub><sup>3-</sup>. The characteristic adsorption at 3572 cm<sup>-1</sup> and 633 cm<sup>-1</sup> are corresponding to OH<sup>-</sup> group of HA powder [20]. The presence of GS were not observed in the FTIR spectra of the HA-GS composite powder and coatings, which might be due to

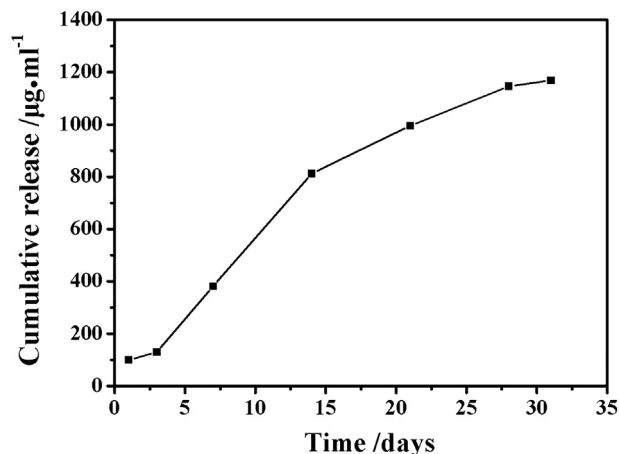


Fig. 5. Cumulative releases of GS from the HA-GS coating *in vitro*.

the small quantity of GS in the composite powder and coatings or the masking of low-intensity resonances of GS by the HA resonances. Similar result was reported [31]. Nevertheless, it is worthwhile to note that almost identical FTIR peaks are shown for the powder and corresponding coatings (Fig. 2), suggesting unique advantages of excellent control over the chemistry of the antibiotic-loaded nanocoatings offered by the VCS.

To further confirm the successful introduction of GS into the HA-GS

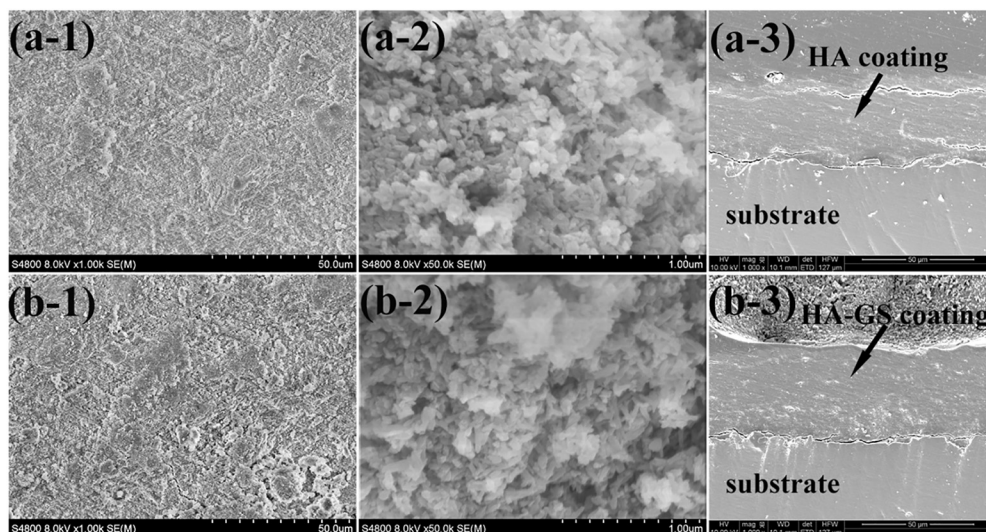


Fig. 4. FE-SEM images of (a) the HA coating and (b) the HA-GS coating. (–1 is enlarged view of selected area in –1, –3 is cross-sectional view of the coating).

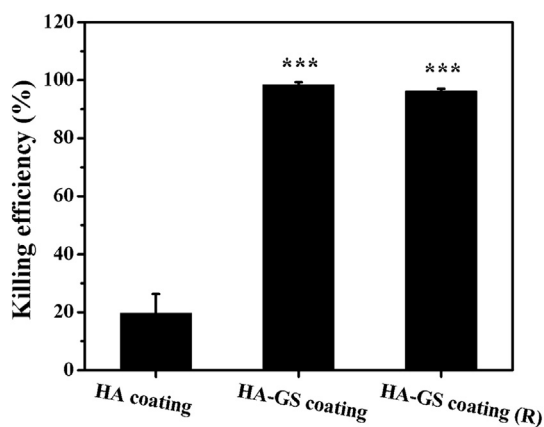


Fig. 6. Antibacterial rates of *E. coli* for the HA coating, the HA-GS coating and the HA-GS coating (R) (the HA-GS coating after incubated in PBS for 31 days).

composite powder and coatings, XPS analysis was performed. Fig. 3 shows the XPS spectra of the HA powder, the HA-GS powder, HA coating and the HA-GS coating. The quantitative data acquired from the XPS detection are listed in Table 1. XPS spectra of the HA powder and the HA coating exhibit the peaks for elements O, Ca and C. For the HA-GS powder and the HA-GS coating, an additional peak around 399 eV for the N element was observed from high resolution XPS spectra (Fig. 3 b), which is derived from amino groups of GS molecules [32]. Although the presence of the peak of N element is not clear in the high resolution XPS spectra of the HA-GS composite powder and coating, the content of N at 1.93% suggests the successful loading of GS into the coating (Table 1). Since the experiments were carried out under air condition, the high C content in the composite coating might result from atmosphere CO<sub>2</sub>. Similar result was reported [31,33]. The result once again confirms that the HA-GS coatings were successfully fabricated.

FESEM views from top surfaces of the coatings (Fig. 4) show similar microstructural features with relatively rough topographical morphologies for the coatings with/without addition of GS. In addition, nanostructured HA particles which are similar to the starting rod-like HA feedstock can be clearly seen on the surfaces of the coatings (Fig. 4 a-2 and b-2). The special hybrid structure comprising both microstructure and nanostructure might play crucial roles in promoting protein interaction and cell responses [34]. It is noted that the morphologies could

be generally observed during the cold spray processing, owing to the fact that cold sprayed coatings are composed of individual particles accomplished by tamping effect [25]. The cross-sectional morphologies of the coatings show a thickness of ~40 μm and suggest a dense structure (Fig. 4 a-3 and b-3). This phenomenon could be explained by the high speed impingement and plastic deformation of particles during the VCS process, resulting in strong adhesion and cohesion [25].

### 3.2. Cumulative release of GS from the coatings and their antibacterial properties

Long-term release of antibiotic from the coatings is essential for the application of antibacterial biomaterials. The release of GS from the HA-GS coatings in PBS solution was measured using UV–vis spectrophotometer, as shown in Fig. 5. It is noted that the HA-GS coatings facilitated long-term release of GS, even after the samples immersed in PBS for 31 days.

In this study, the model gram-negative bacterium *E. coli* were used to evaluate the antibacterial properties of the samples (Fig. 6). Titanium substrates were used as controls. The antibacterial rate of the HA coatings was around 19.6%. The antibacterial rate of the as-sprayed HA-GS coatings was significantly improved to around 99%, mainly due to the good antibacterial property of GS [9]. Although the antibacterial rates of the HA-GS coatings after immersed in PBS for 31 days (the HA-GS(R) coating) showed a slight decrease, favorable antibacterial property was still observed, since the HA-GS coatings showed long-term release of GS. Therefore, the results of both gentamicin measurement and antibacterial test confirm that the gentamicin released was still bioactive. This result implies that coating fabrication by VCS with antibacterial agent-incorporated HA composite might open a new window for producing antibacterial biomedical materials.

### 3.3. Biocompatibility of the coatings

Favorable biocompatibility is essentially required for potential applications of the HA-GS composite coatings. To examine the biocompatibility of the coatings, human osteoblasts were grown on different samples for 1 and 3 days and analyzed by SEM (Fig. 7). It was found that cells showed a similar flattened and well spreading morphology on the surfaces of the titanium substrates, the HA coating and the HA-GS coating after culture for 1 day (Fig. 7 a-1, b-1 and c-1). The average number of cells adhered to the HA coating was higher than

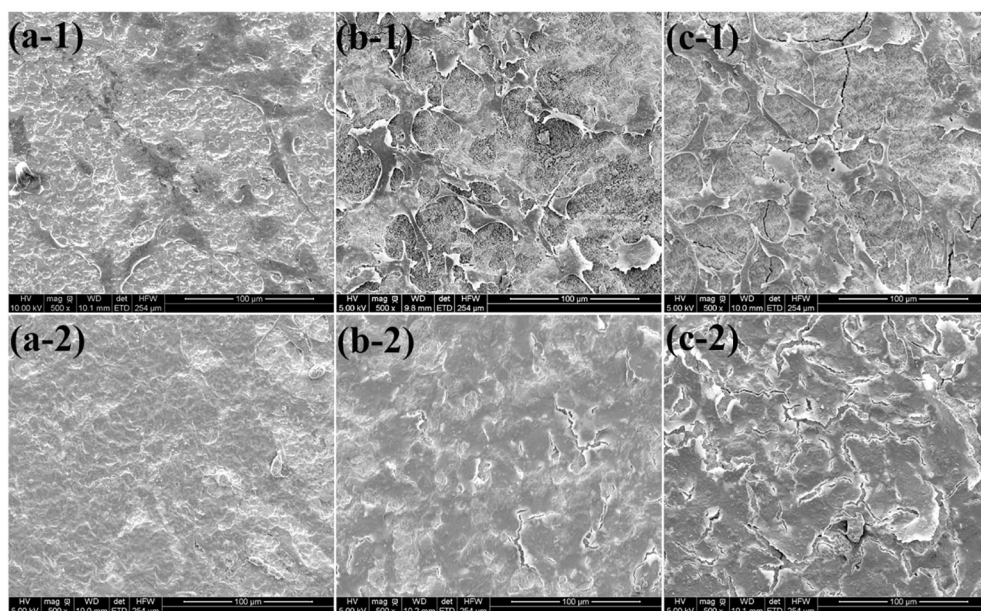


Fig. 7. FE-SEM micrographs of human osteoblasts cultured on the surfaces of (a) the Ti substrate, (b) the HA coating, and (c) the HA-GS coating for 1 day (– 1) and 3 days (– 2).

those of the titanium substrates, suggesting better biocompatibility of the HA coatings. Furthermore, the number and morphology of cells cultured on the HA-GS coating was similar to those on the HA coating. In addition, overall samples were fully covered by cells after cultured for 3 days, indicating outstanding biocompatibility of the HA-GS coating. Taken together, we have successfully deposited the HA-GS composite coating onto titanium substrate that displayed a long-term antibacterial property and excellent biocompatibility.

#### 4. Conclusions

In this study, HA-GS composite coatings were constructed by VCS on titanium substrates with the successful incorporation of GS. Comprehensive characterization showed that the physical and chemical characteristics of the as-synthesized composite powder were completely retained in the as-deposited coatings. The GS-containing HA coating was further confirmed to show a long-term antibacterial property and favorable biocompatibility. The construction of the novel HA-GS composite antibacterial coatings by the VCS approach might facilitate the development of long-term drug-releasing coatings for medical implants with exceptional properties in the future.

#### Acknowledgements

This work was supported by National Natural Science Foundation of China (grant # 51401232 and 41706076), CAS-Iranian Vice Presidency for Science and Technology Joint Research Project (grant # 174433KYSB20160085), and Ningbo Municipal Major Projects on Industrial Technology Innovation (grant # 2015B11054).

#### References

- [1] W. Liu, J. Chang, *In vitro* evaluation of gentamicin release from a bioactive tricalcium silicate bone cement, *Mat. Sci. Eng. C-Mater.* 29 (2009) 2486–2492.
- [2] X. Chen, K. Cai, J. Fang, M. Lai, Y. Hou, J. Li, Z. Luo, Y. Hu, L. Tang, Fabrication of selenium-deposited and chitosan-coated titania nanotubes with anticancer and antibacterial properties, *Colloid. Surf. B* 103 (2013) 149–157.
- [3] J.H. Chu, J. Lee, C.C. Chang, Y.C. Chan, M.L. Liou, J.W. Lee, J.S.C. Jang, J.G. Duh, Antimicrobial characteristics in Cu-containing Zr-based thin film metallic glass, *Surf. Coat. Technol.* 259 (2014) 87–93.
- [4] H.I. Chang, Y.C. Lau, C. Yan, A.G.A. Coombes, Controlled release of an antibiotic, gentamicin sulphate, from gravity spun polycaprolactone fibers, *J. Biomed. Mater. Res. A* 84A (2008) 230–237.
- [5] K.C. Popat, M. Eltgroth, T.J. Latempa, C.A. Grimes, T.A. Desai, Decreased staphylococcus epidermis adhesion and increased osteoblast functionality on antibiotic-loaded titania nanotubes, *Biomaterials* 28 (2007) 4880–4888.
- [6] R. Cristescu, C. Popescu, G. Socol, A. Visan, I.N. Mihailescu, S.D. Gittard, P.R. Miller, T.N. Martin, R.J. Narayan, A. Andronie, I. Stamatina, D.B. Chrisey, Deposition of antibacterial poly(1,3-bis-(p-carboxyphenoxy propane)-co-(sebacic anhydride)) 20:80/gentamicin sulfate composite coatings by maple, *Appl. Surf. Sci.* 257 (2011) 5287–5292.
- [7] Z.S. Nurkeeva, V.V. Khutoryanskiy, G.A. Mun, M.V. Sherbakova, A.T. Ivaschenko, N.A. Aitkhozhina, Polycomplexes of poly(acrylic acid) with streptomycin sulfate and their antibacterial activity, *Eur. J. Pharm. Biopharm.* 57 (2004) 245–249.
- [8] L.D. Silverman, L. Lukashova, O.T. Herman, J.M. Lane, A.L. Boskey, Release of gentamicin from a tricalcium phosphate bone implant, *J. Orthop. Res.* 25 (2007) 23–29.
- [9] E. Wers, H. Oudadesse, B. Lefevre, O. Merdignac-Conanec, A. Barroug, Evaluation of the kinetic and relaxation time of gentamicin sulfate released from hybrid biomaterial bioglass-chitosan scaffolds, *Appl. Surf. Sci.* 353 (2015) 200–208.
- [10] A. Rudin, C.A. Phillips, D.W. Gump, B.R. Forsyth, Antibacterial activity of gentamicin sulfate in tissue culture, *Appl. Microbiol.* 20 (1970) 989–990.
- [11] P. Frutos Cabanillas, E. Diez Pena, J.M. Barrales-Rienda, G. Frutos, Validation and *in vitro* characterization of antibiotic-loaded bone cement release, *Int. J. Pharm.* 209 (2000) 15–26.
- [12] W.C. Liu, C.T. Wong, M.K. Fong, W.S. Cheung, R.Y.T. Kao, K.D.K. Luk, W.W. Lu, Gentamicin-loaded strontium-containing hydroxyapatite bioactive bone cement-an efficient bioactive antibiotic drug delivery system, *J. Biomed. Mater. Res. B* 95B (2010) 397–406.
- [13] E. Diez Pena, G. Frutos, P. Frutos, J.M. Barrales-Rienda, Gentamicin sulphate release from a modified commercial acrylic surgical radiopaque bone cement. I. influence of the gentamicin concentration on the release process mechanism, *Chem. Pharm. Bull.* 50 (2002) 1201–1208.
- [14] G. Ginalska, M. Osinska, A. Uryniak, T. Urbanik Sypniewska, A. Belcarz, W. Rzeski, A. Wolski, Antibacterial activity of gentamicin-bonded gelatin-sealed polyethylene terephthalate vascular prostheses, *Eur. J. Vasc. Endovasc.* 29 (2005) 419–424.
- [15] H. Pandey, V. Parashar, R. Parashar, R. Prakash, P.W. Ramteke, A.C. Pandey, Controlled drug release characteristics and enhanced antibacterial effect of graphene nanosheets containing gentamicin sulfate, *Nano* 3 (2011) 4104–4108.
- [16] M. Yoshinari, Y. Oda, T. Kato, K. Okuda, Influence of surface modifications to titanium on antibacterial activity *in vitro*, *Biomaterials* 22 (2001) 2043–2048.
- [17] C. Moseke, F. Hage, E. Vorndran, U. Gbureck, TiO<sub>2</sub> nanotube arrays deposited on Ti substrate by anodic oxidation and their potential as a long-term drug delivery system for antimicrobial agents, *Appl. Surf. Sci.* 258 (2012) 5399–5404.
- [18] V. Uskokovic, Nanostructured platforms for the sustained and local delivery of antibiotics in the treatment of osteomyelitis, *Crit. Rev. Ther. Drug* 32 (2015) 1–59.
- [19] H. Duan, Y. Ma, X. Liu, L. Hao, N. Zhao, Hierarchically nanostructured hydroxyapatite microspheres as drug delivery carriers and their effects on cell viability, *RSC Adv.* 5 (2015) 83522–83529.
- [20] Y. Liu, J. Huang, H. Li, Synthesis of hydroxyapatite-reduced graphite oxide nanocomposites for biomedical applications: oriented nucleation and epitaxial growth of hydroxyapatite, *J. Mater. Chem. B* 1 (2013) 1826–1834.
- [21] Y. Liu, Z. Dang, Y. Wang, J. Huang, H. Li, Hydroxyapatite/graphene-nanosheet composite coatings deposited by vacuum cold spraying for biomedical applications: Inherited nanostructures and enhanced properties, *Carbon* 67 (2014) 250–259.
- [22] L. Sun, C.C. Berndt, K.A. Gross, A. Kucuk, Material fundamentals and clinical performance of plasma-sprayed hydroxyapatite coatings: a review, *J. Biomed. Mater. Res.* 58 (2001) 570–592.
- [23] J. Akedo, Room temperature impact consolidation (RTIC) of fine ceramic powder by aerosol deposition method and applications to microdevices, *J. Therm. Spray Technol.* 17 (2008) 181–198.
- [24] S.D. Cook, K.A. Thomas, J.F. Kay, M. Jarcho, Hydroxyapatite-coated titanium for orthopedic implant applications clinical orthopaedics and related research, *Clin. Orthop. Relat. R.* (1988) 225–243.
- [25] Y. Liu, Y.Y. Wang, G.J. Yang, J.J. Feng, K. Kusumoto, Effect of nano-sized TiN additions on the electrical properties of vacuum cold sprayed SiC coatings, *J. Therm. Spray Technol.* 19 (2010) 1238–1243.
- [26] S.Q. Fan, G.J. Yang, C.J. Li, G.J. Liu, C.X. Li, L.Z. Zhang, Characterization of microstructure of nano-TiO<sub>2</sub> coating deposited by vacuum cold spraying, *J. Therm. Spray Technol.* 15 (2006) 513–517.
- [27] G.A. Buckholtz, N.A. Reger, W.D. Anderton, P.J. Schimoler, S.L. Roudebush, W.S. Meng, M.C. Miller, E.S. Gwalt, Reducing *Escherichia coli* growth on a composite biomaterial by a surface immobilized antimicrobial peptide, *Mater. Sci. Eng. C* 65 (2016) 126–134.
- [28] Z. Li, D. Lee, X. Sheng, R.E. Cohen, M.F. Rubner, Two-level antibacterial coating with both release-killing and contact-killing capabilities, *Langmuir* 22 (2006) 9820–9823.
- [29] K.D. Park, Y.S. Kim, D.K. Han, Y.H. Kim, E.H.B. Lee, H. Suh, K.S. Choi, Bacterial adhesion on PEG modified polyurethane surfaces, *Biomaterials* 19 (1998) 851–859.
- [30] X. Chen, K. Cai, J. Fang, M. Lai, J. Li, Y. Hou, Z. Luo, Y. Hu, L. Tang, Dual action antibacterial TiO<sub>2</sub> nanotubes incorporated with silver nanoparticles and coated with a quaternary ammonium salt (QAS), *Surf. Coat. Technol.* 216 (2013) 158–165.
- [31] X. Cui, Y. Gu, L. Li, H. Wang, Z. Xie, S. Luo, N. Zhou, W. Huang, M.N. Rahaman, *In vitro* bioactivity, cytocompatibility, and antibiotic release profile of gentamicin sulfate-loaded borate bioactive glass/chitosan composites, *J. Mater. Sci.-Mater. Med.* 24 (2013) 2391–2403.
- [32] D.W. Lee, Y.P. Yun, K. Park, S.E. Kim, Gentamicin and bone morphogenic protein-2 (BMP-2)-delivering heparinized-titanium implant with enhanced antibacterial activity and osteointegration, *Bone* 50 (2012) 974–982.
- [33] D. Chen, Z. Jiang, J. Geng, Q. Wang, D. Yang, Carbon and boron Co-doped TiO<sub>2</sub> with enhanced visible-light photocatalytic activity, *Ind. Eng. Chem. Res.* 46 (2007) 2741–2746.
- [34] T.J. Webster, C. Ergun, R.H. Doremus, R.W. Siegel, R. Bizios, Specific proteins mediate enhanced osteoblast adhesion on nanophase ceramics, *J. Biomed. Mater. Res.* 51 (2000) 475–483.